Supporting Information

Impact of the Mechanical Properties of a Functionalized Cross-linked Binder on the Longevity of Li-S Batteries

C. Y. Kwok,[a] *Q. Pang*,[a] *A. Worku*,[b] *X. Liang*,[a] *M. Gauthier*,[b*] *L. F. Nazar*[a*]

[a]Waterloo Institute of Nanotechnology and Department of Chemistry, University of Waterloo, 200 University Ave. W., Waterloo, Ontario, N2L 3G1, Canada

[b]Department of Chemistry, University of Waterloo, 200 University Ave. W., Waterloo, Ontario, N2L 3G1, Canada

[*] Correspondence to be addressed to L. F. Nazar (e-mail: lfnazar@uwaterloo.ca) or M. Gauthier (e-mail: gauthier@uwaterloo.ca)

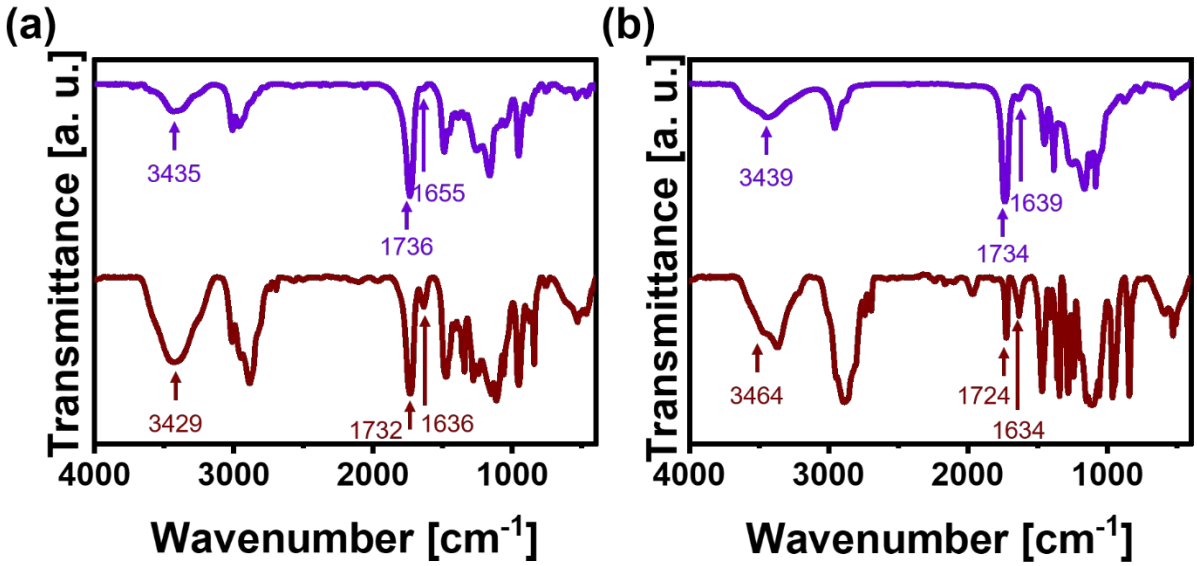

Figure S1. FTIR transmission spectra for (**a**) poly(AETMAC-*co*-EGDA) and (**b**) poly(DADMAC-*co*-EGDA), respectively, to confirm cross-linking: physical mixture of their homopolymer counterparts (burgundy), and the cross-linked polymer (purple).

Discussion of Figure S1. The successful cross-linking copolymerization to produce poly(AETMAC-*co*-EGDA) and poly(DADMAC-*co*-EGDA) is confirmed by their FTIR spectra (**Figure S1, purple curve**) where an absence of alkene (C=C or =CH) bands in the materials is noted. This suggests a complete conversion of the precursor monomer, where the residual monomers were washed away in the purification steps. Instead, the spectrum in **Figure S1a** exhibits ester C=O (1736 cm^{-1}) and C-N (1655 and 3435 cm^{-1}) moitiés.[1] Furthermore, compared with the FTIR spectrum of the physical mixture of poly(AETMAC)-poly(EGDA) homopolymer material (**Figure S1a, burgundy curve**), the band attributed to the C-N stretching vibration in the secondary amine group and the C=O stretching band in the ester group are shifted from 3429 to 3435 cm^{-1} and 1732 to 1736 cm^{-1}, respectively, indicative of strong bonding interactions within the polymer due to the copolymerization linkage.

Similarly, the successful cross-linking of DADMAC by EGDA to form poly(DADMAC-*co*-EGDA) was also confirmed by FTIR (**Figure S1b, purple curve**): peaks attributed to poly(DADMAC-*co*-EGDA): are ester C=O (1734 cm^{-1}) and C-N (1639 and 3439 cm^{-1}) groups.[2] The characteristic peaks ascribed to the C-N and C=O groups in poly(DADMAC-*co*-EGDA) are also significantly shifted compared to their homopolymer mixture (**Figure S1b, burgundy curve**).

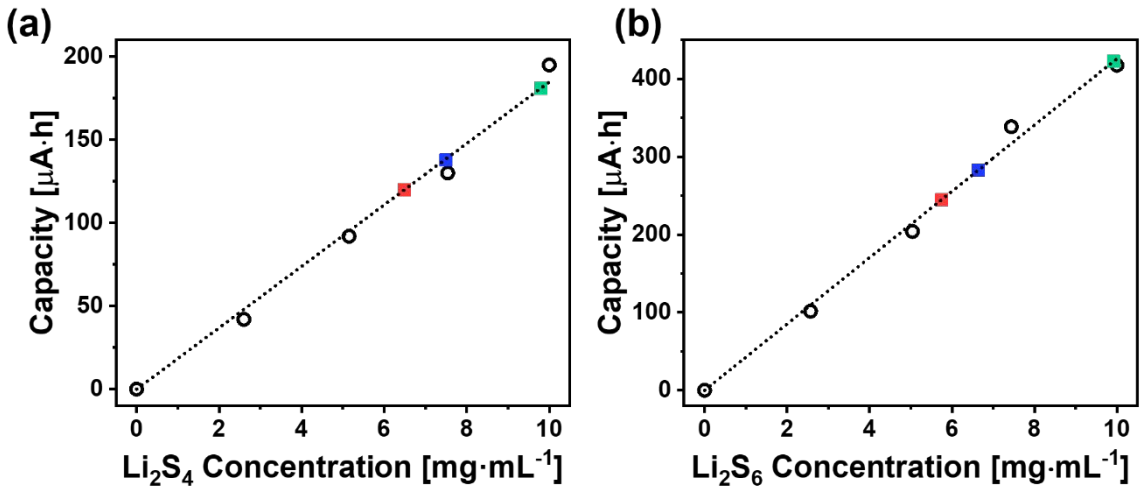

Figure S2. Calibration plot (open circles) derived from the capacity by oxidizing a known concentration of (**a**) Li_2S_4 and (**b**) Li_2S_6 in DME to sulfur. Experimental points (solid squares) were mapped on the curve for poly(AETMAC-*co*-EGDA) (red), poly(DADMAC-*co*-EGDA) (blue), and PVdF (green) using the same method, providing a quantitative metric for their polysulfide adsorptivity.

Discussion of Figure S2. A total of five calibration solutions and three polymeric binder materials were analyzed for each lithium polysulfide. The capacity achieved for all calibration and sample solutions are plotted ($R^2_{Li2S4} = 0.998$ and $R^2_{Li2S6} = 0.999$).

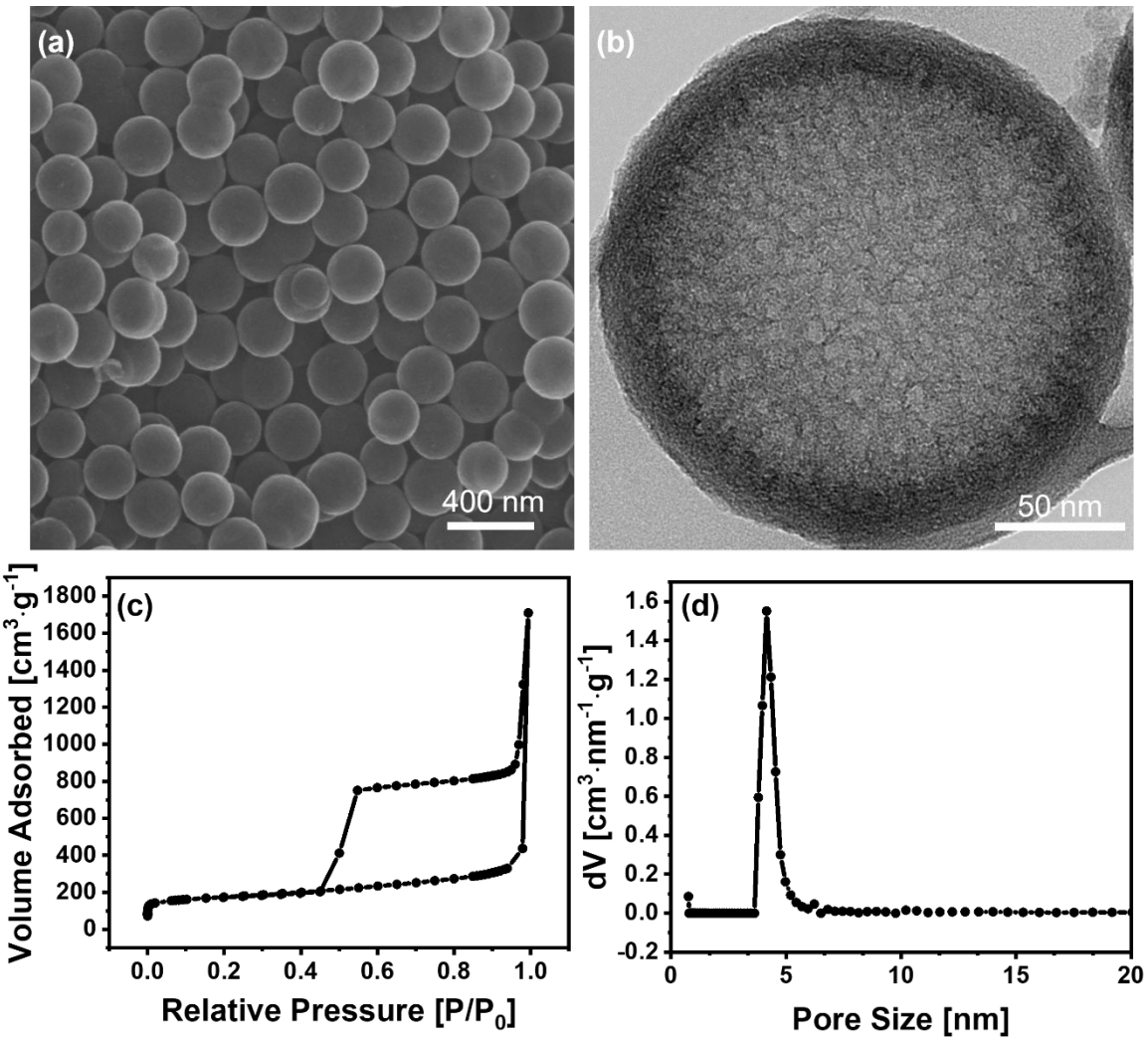

Figure S3. (**a**) SEM and (**b**) TEM images of the porous hollow carbon spheres (PHCS). (**c**) N_2 adsorption isotherm and (**d**) pore size distribution curve for the same material.

Discussion of Figure S3. Scanning electron microscopy (SEM; **Figure S3a**) and transmission electron microscopy (TEM; **Figure S3b**) confirm that the nanoparticles were homogenous with average size of ~200 nm. The specific surface area of the PHCSs, measured by nitrogen adsorption analysis, is 593 $m^2 \cdot g^{-1}$ with a pore volume of 1709 $cm^3 \cdot g^{-1}$ (**Figure S3c-d**).

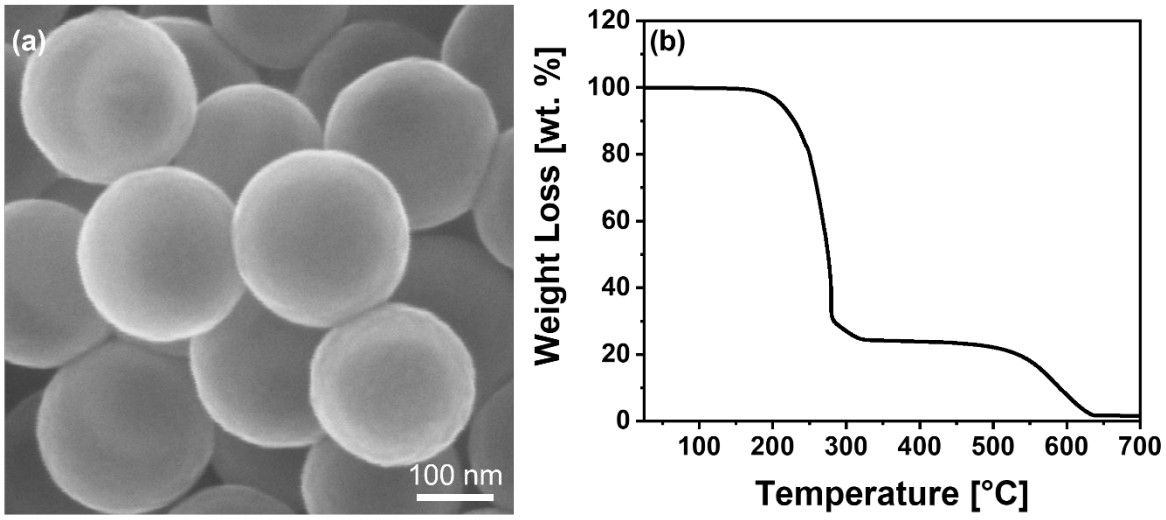

Figure S4. (**a**) SEM image for S-PHCS. (**b**) TGA curve for the S-PHCS composite, yielding a sulfur content of 75 wt. % at a ramp rate of 10 °C·min^{-1} under air flow.

Discussion of Figure S4. The SEM image in **Figure S4a** shows that sulfur is uniformly distributed to afford the composite material S-PHCSs, and no bulk sulfur deposits are visible. Thermogravimetric analysis (TGA, **Figure S4b**) in flowing air further confirms the sulfur loading to be 75 wt. %, and shows two regions of sulfur loss. The 70 wt. % sulfur loss below 280 °C is attributed to sulfur in the mesoporous shell and near the inner surface. At 300 °C, an additional 5 wt. % loss is attributed to sulfur confined deep in the interior structure of the carbon spheres. The weight loss at around 580 °C is due to oxidation of the PHCSs.

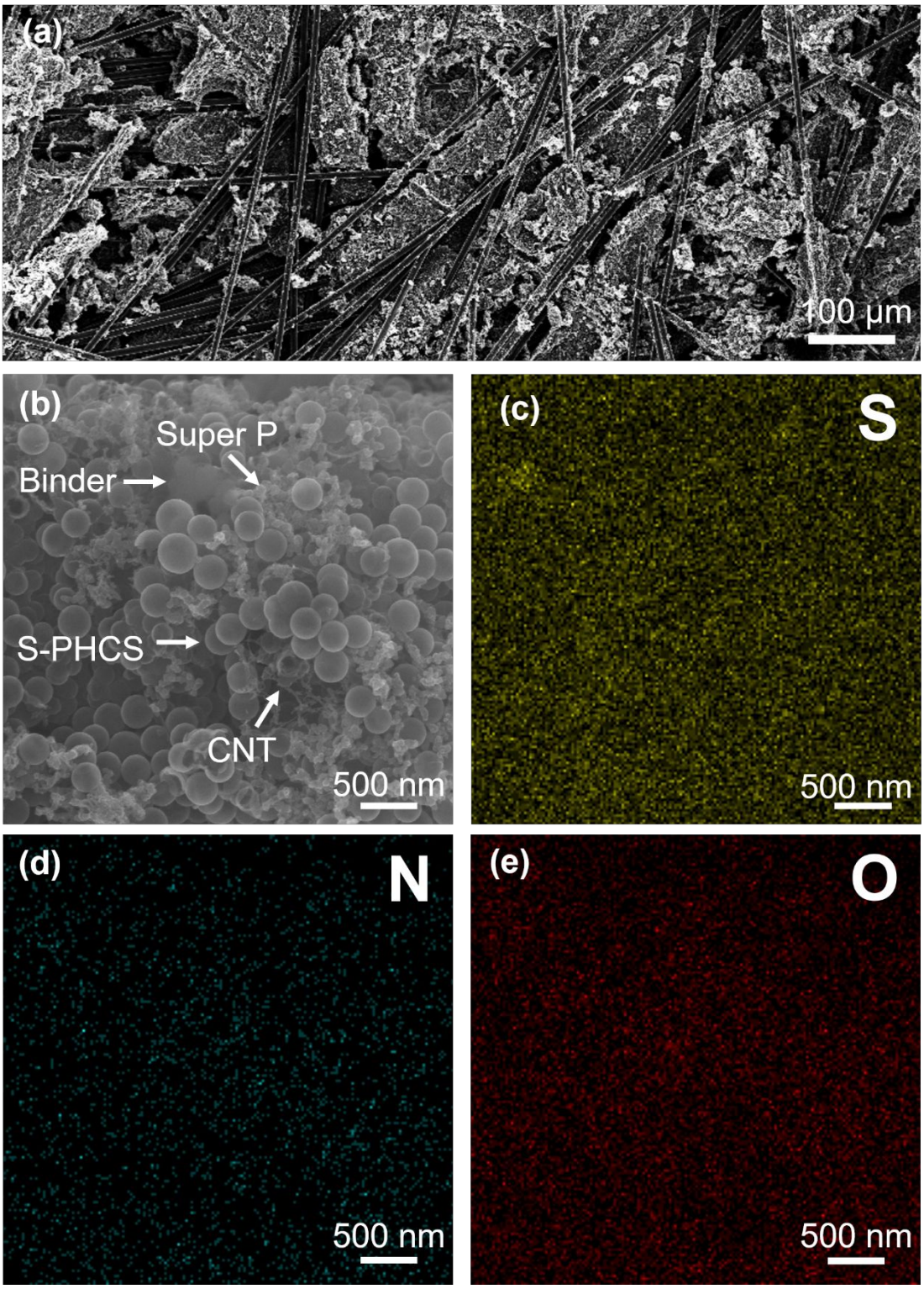

Figure S5. (**a**) SEM image of the P50 carbon paper current collector. (**b-d**) SEM EDAX analysis of the sulfur cathode fabricated with poly(AETMAC-*co*-EGDA). (**b**) SEM image; elemental mapping of (**c**) S; (**d**) **N**; and (**e**) **O**.

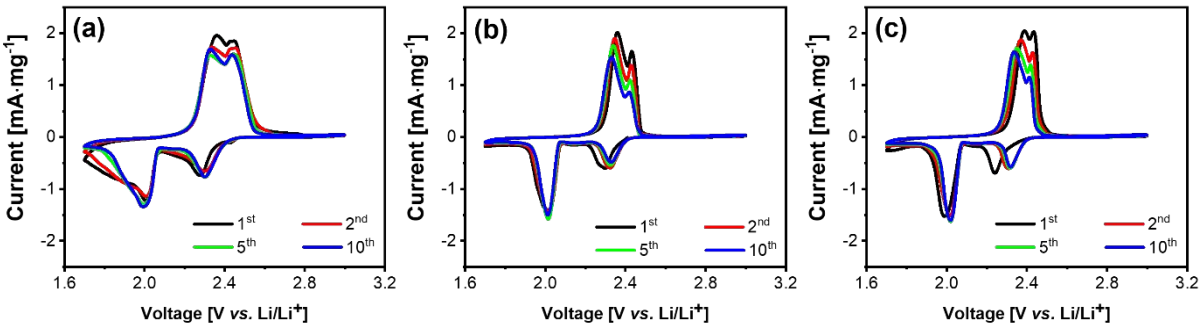

Figure S6. CV profiles conducted at a scan rate of 0.1 mV s^{-1} of the sulfur cathodes fabricated with (**a**) poly(AETMAC-*co*-EGDA), (**b**) poly(DADMAC-*co*-EGDA) and (**c**) PVDF, shown at different sweep cycles. The small reduction in hysteresis between the 1st and subsequent cycles, most evident for PVDF, is ascribed to changes incurred on fully wetting the electrode on the first cycle.

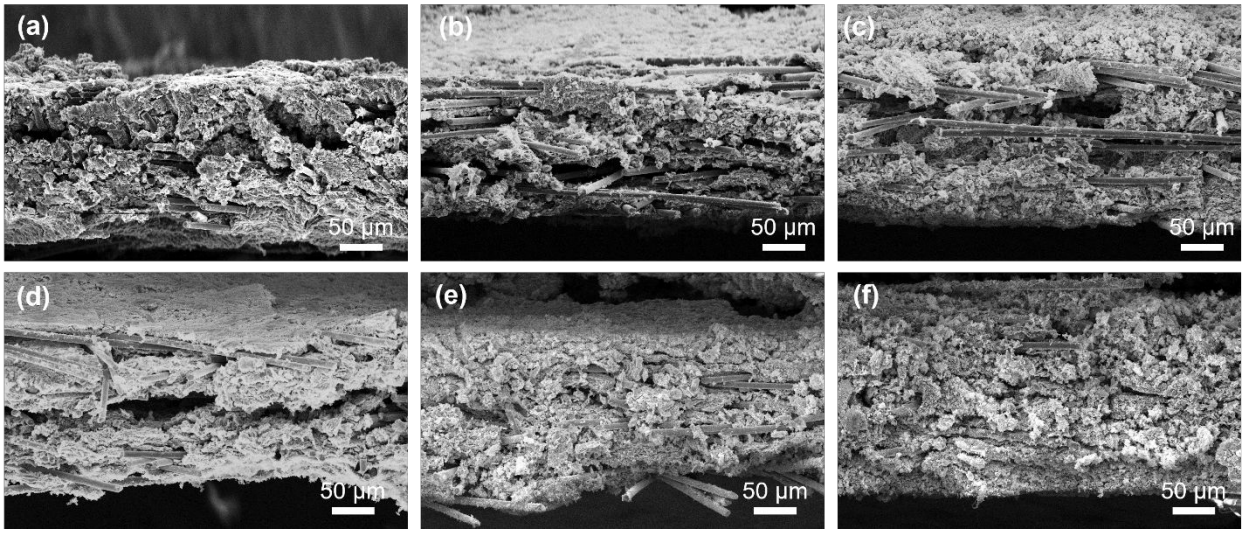

Figure S7. SEM images of the cross-section of the sulfur cathodes (**a-c**) before and (**d-f**) after 10 cycles fabricated with (**a**, **d**) PVDF; (**b**, **c**) poly(DADMAC-*co*-EGDA); and (**c**, **f**) poly(AETMAC-*co*-EGDA).

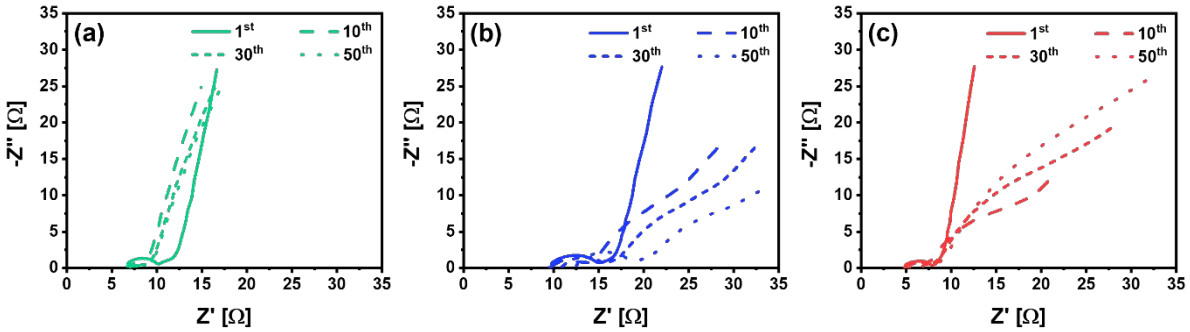

Figure S8. Electrochemical impedance spectroscopy: Nyquist plots of the sulfur cathodes fabricated with (**a**) PVDF, (**b**) poly(DADMAC-*co*-EGDA), and (**c**) poly(AETMAC-*co*-EGDA) at different cycle numbers.

References

(1) Shen, S.; Zhu, Z.; Liu, F. Introduction of Poly[(2-acryloyloxyethyl trimethyl ammonium chloride)-co-(acrylic acid)] Branches onto Starch for Cotton Warp Sizing. *Carbohydr. Polym.*, **2016**, *138*, 280-289.

(2) Aly, M. A. S.; Gauthier, M.; Yeow, J. On-Chip Cell Lysis by Antibacterial Non-Leaching Reusable Quaternary Ammonium Monolithic Column. *Biomed. Microdevices*, **2016**, *18:2*.